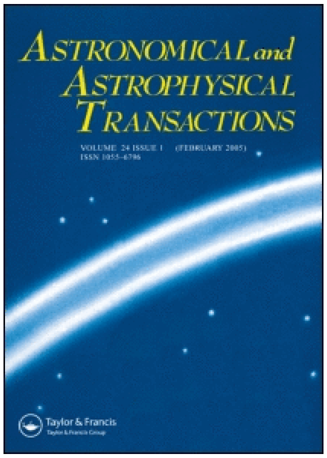

Astronomical & Astrophysical Transactions

The Journal of the Eurasian Astronomical Society

Publication details, including instructions for authors and subscription information:
http://www.informaworld.com/smpp/title~content=t713453505

Quasistationary phenomena in the solar corona

Podgorny; Podgorny; Minami

Online Publication Date: 01 January 2003
To cite this Article: Podgorny, Podgorny and Minami (2003) 'Quasistationary phenomena in the solar corona', Astronomical & Astrophysical Transactions, 22:4, 585 - 591
To link to this article: DOI: 10.1080/1055679031000139442
URL: http://dx.doi.org/10.1080/1055679031000139442

Astronomical and Astrophysical Transactions
Vol. 22, Nos. 4–5, August–October 2003, pp. 585–591

QUASISTATIONARY PHENOMENA IN THE SOLAR CORONA

I. M. PODGORNY[a]*, A. I. PODGORNY[b] and S. MINAMI[c]

[a]Institute for Astronomy, Russian Academy of Science, Moscow 109017, Russia;
[b]P.N. Lebedev Physical Institute, Russian Academy of Science, Moscow 119991, Russia;
[c]Osaka City University, Osaka 558, Japan

(Received October 5, 2002)

Postflare loops, which fill by hot plasma from chromospheric sources, are numerically simulated. The PERESVET code is used to solve the system of resistive magnetohydrodynamic equations. The possible mechanisms of plasma heating in the loop are discussed. It is shown that plasma heating can be produced by magnetic line reconnection. The stable plasma confinement in the arch magnetic field of the solar corona is determined by field-aligned current generation.

Keywords: Sun; post-flare loops; solar corona

1 INTRODUCTION

Bright loops aligned with magnetic lines can reach a height of about 10^{10} cm. Often, the loop thickness does not exceed 5×10^8 cm. A typical plasma density is 10^8–10^{10} cm^{-3}, and the temperature reaches approximately 1000 eV. Usually the outer part of the loop is hotter than its inner part (Schmieder et al., 1996).

The loops are anchored in the chromosphere, which most likely is the source of the dense plasma in the loops. The ejection of highly ionized matter from the chromosphere hot source has been demonstrated (Fisher et al., 1985). Culhane et al. (1991) proposed that such impulsive chromospheric evaporation appears because of the energy from fast electrons precipitated into the chromosphere during a flare. According to the flare electrodynamic model (Podgorny and Podgorny, 2001a), fast electrons are accelerated in the upward field-aligned currents (FACs). As a result, two centres of chromospheric evaporation, which inject hot plasma into the legs of the loop, can be generated. The plasma streams upwards and fills the magnetic tube. This pattern of postflare formation has been confirmed in numerical magnetohydrodynamic (MHD) simulation (Podgorny and Podgorny, 2002).

There are two fundamental problems associated with another quasistationary phenomena in the solar corona: the X-ray bright point (XBP) (the source of local heating of the corona) and the long existence of very hot plasma (of the order of 10 h) in a small restricted region in

* Corresponding author. E-mail: podgorny@rssi.inasan.ru

ISSN 1055-6796 print; ISSN 1476-3540 online
DOI: 10.1080/1055679031000139442

spite of the high thermal corona conductivity. Typical XBP parameters are as follows: the point diameter is $d \approx 5 \times 10^8$ cm, the plasma temperature is $T \approx 1000$ eV, the density is $n \approx 10^9\,cm^{-3}$, and the lifetime is of the order of 10 h. Numerical MHD experiments (Podgorny and Podgorny, 2001b) have shown that effective magnetic thermal isolation and plasma confinement are supplied in the vicinity of a neutral line. Plasma heating is produced by magnetic reconnection at weak MHD disturbances arriving from the photosphere.

Here we present results concerning plasma heating in loops and its stable confinement in a configuration that is unstable in laboratory conditions. Anisotropy of the plasma thermal conductivity in the magnetic field and FAC generation are taken into account.

2 NUMERICAL METHODS

The system of MHD equations for compressible plasma with all dissipative terms is solved numerically in a dimensionless form:

$$\frac{\partial B}{\partial t} = \mathrm{rot}(V \times B) - \frac{1}{Re_m}\mathrm{rot}\left(\frac{\sigma_0}{\sigma}\ \mathrm{rot}\,B\right), \tag{1}$$

$$\frac{\partial \rho}{\partial t} = -\mathrm{div}(V\rho), \tag{2}$$

$$\frac{\partial V}{\partial t} = -(V, \boldsymbol{\nabla})V - \frac{\beta_0}{2\rho}\boldsymbol{\nabla}(\rho T) - \frac{1}{\rho}(B \times \mathrm{rot}\,B) + \frac{1}{Re\,\rho}\ \Delta V + G_g G, \tag{3}$$

$$\frac{\partial T}{\partial t} = -(V, \boldsymbol{\nabla})T - (\gamma - 1)T\ \mathrm{div}\ V + (\gamma - 1)\frac{2\sigma_0}{Re_m\ \sigma\beta_0\rho}(\mathrm{rot}\ B)^2 - (\gamma - 1)G_q\rho L'(T)$$
$$+\frac{\gamma - 1}{\rho}\ \mathrm{div}(e_{\|}\kappa_{dl}(e_{\|}, \boldsymbol{\nabla}T) + e_{\perp 1}\kappa_{\perp dl}(e_{\perp 1}, \boldsymbol{\nabla}T) + e_{\perp 2}\kappa_{\perp dl}(e_{\perp 2}, \boldsymbol{\nabla}T)). \tag{4}$$

The unit of the length L_0 is taken as the size of calculation region $0 \le x \le 1$, $0 \le y \le 1$, $0 \le z \le 1$. The Y axis is directed perpendicular to the solar surface; the plane of photosphere is X–Z ($y = 0$). The unit of the magnetic field B_0 is taken as the field value above the active region. The units of the plasma density ρ_0 and temperature T_0 are taken as their initial values, which are accepted as constant in space. The units of the plasma velocity, time, current density and dipole moment are taken as the Alfvén velocity $V_0 = V_A = B_0/(4\pi\rho_0)^{1/2}$, $t_0 = L_0/V_0$, $j_0 = cB_0/4\pi L_0$ and $M_0 = B_0 L_0^3$, respectively.

In equations (1)–(4), $Re_m = V_0 L_0/\nu_{m0}$ is the magnetic Reynolds number, $\nu_{m0} = c^2/4\pi\sigma_0$ is the magnetic viscosity for the conductivity σ_0 at the temperature T_0, σ is conductivity given by $\sigma/\sigma_0 = T^{3/2}$, and $\beta = 8\pi n_0 k T_0/B_0^2$ ($n_0 = \rho_0/m_i$, where m_i is the ion mass). $Re = \rho_0 L_0 V_0/\eta$ is the Reynolds number, where η is the viscosity. $G_q = L(T_0)\rho_0 t_0/T_0$, where $L(T_0)$ is the Cox and Tucker radiation function for the ionization equilibrium of solar corona. $L'(T) = L(T_0 T)/L(T_0)$ is the dimensionless radiation function. $e_{\|}$, $e_{\perp 1}$ and $e_{\perp 2}$ are the orthogonal unit vectors that are parallel, perpendicular and perpendicular respectively to the magnetic field. $\kappa_{d1} = \kappa/\Pi\kappa_0$ is the dimensionless thermal conductivity along the magnetic field lines, where $\Pi = \rho_0 L_0 V_0/\kappa_0$ is the Peclet number, κ_0 is the thermal conductivity for the temperature T_0, and κ is the thermal conductivity given by $\kappa/\kappa_0 = T^{5/2}$. $\kappa_{\perp dl} = (\kappa\kappa_0^{-1}\Pi^{-1})(\kappa_B\kappa_{0B}^{-1}\Pi_B^{-1})/[(\kappa\kappa_0^{-1}\Pi^{-1}) + (\kappa_B\kappa_{0B}^{-1}\Pi_B^{-1})]$ is the dimensionless thermal conductivity perpendicular to the magnetic field lines, where $\Pi_B = \rho_0 L_0 V_0/\kappa_{0B}$ is the Peclet number for the thermal conductivity κ_{0B} (for T_0, ρ_0 and B_0) across the strong magnetic field. $\kappa_B/\kappa_{0B} = \rho^2 B^{-2} T^{-1/2}$. $G_g G$ is the dimensionless gravitational acceleration.

To solve the MHD equation the PERESVET code (Podgorny and Podgorny, 2001a, 2002) is used. The finite-difference scheme is absolutely implicit; it is solved by the method of iterations. The numerical method includes multilevel division of the time step in the regions where there is a large gradient of values. These properties of the scheme permit us to stabilize most of the numerical instabilities.

In our calculations the parameters are chosen according to the principle of limited simulation: $\gamma = 5/3$, $\mathrm{Re_m} = 10^5$, $\mathrm{Re} = 10^4$, $\beta = 2 \times 10^{-5}$, $\Pi = 100$, $\Pi_\mathrm{B} = 10^8$ and $\mathrm{G_q} = 10^{-4}$. The gravitational force can be neglected in comparison with the magnetic and plasma pressure forces: $\mathrm{G_g} = 0$.

For $\mathrm{B_0} = 300\,\mathrm{G}$ and $\mathrm{n} \approx 10^8\,\mathrm{cm\,s^{-1}}$, the Alfvén velocity is $6 \times 10^9\,\mathrm{cm\,s^{-1}}$. For $\mathrm{L} = 10^{10}$ the dimensionless unit of time corresponds to 2 s.

3 CHROMOSPHERIC EVAPORATION

The following scenario of loop filling by a dense plasma is numerically simulated. According to the electrodynamic solar flare model (Podgorny and Podgorny, 2001a) (Fig. 1) a vertical current sheet (CS) appears in the vicinity of a neutral line because of focusing disturbances that arrive from the photosphere. The energy accumulated in the CS magnetic field is released on CS decay, producing a flare. The loop is produced during flare development. The thin lines are the magnetic field lines. The Hall electric field $\mathrm{E} = \mathrm{j} \times \mathrm{B}/\mathrm{nec}$ is generated along the CS. The Hall field produces FACs in the corona. The FACs are shown as thick curves. Upward and downward FACs are enclosed in the chromosphere by Pedersen currents. Electrons accelerated in the upward current precipitate in the chromosphere. Effective electron acceleration in the FACs can appear in a potential discontinuity or double electric layers. The fast electron precipitation produces visible and X-ray luminosities and local centres of chromosphere heating that act as sources of chromospheric evaporation.

During CS decay the new magnetic lines arrive at the CS from the right- and from the left-hand sides and reconnect in the sheet. The places where electrons are accelerated along the FACs move apart. As a result, flare ribbons also move apart. This behaviour of the ribbons is rather typical. After CS decay and the initial magnetic configuration has been restored, hot

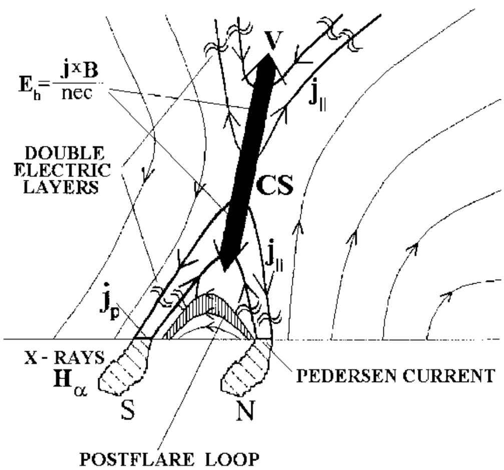

FIGURE 1 The solar flare electrodynamic model. The thick lines show FACs.

chromospheric sources occur inside the arc magnetic field. The effect of plasma ejection from such sources is the topic of MHD numerical experiments.

In the numerical experiment the magnetic field is produced by four vertical magnetic dipoles placed under the photosphere (Fig. 2(a)). Their magnetic moments and positions are as follows: $\mu_1 = 26.3$ at $X = 0.75$ and $Y = -1.5$; $\mu_2 = -48.1$ at $X = 0.25$ and $Y = -1.5$; $\mu_3 = 48.2$ at $X = 0$ and $Y = -1.5$; $\mu_4 = 26.25$ at $X = 1$ and $Y = -1.5$. This field contains a neutral line above the photosphere. The cross indicates the point where the X–Y is intersected by the neutral line. Podgorny and Podgorny (2001c) showed that, in the vicinity of such neutral line, a vertical CS appears as a result of disturbance focusing. The disturbance arrives from the photosphere. The energy accumulated in the magnetic field of the CS can be released, producing a solar flare.

The plasma density $\rho = 2000$ and temperature $T = 10$ have been used for the sources. The source positions are shown in Figure 2(a). The plasma flow from sources does not disturb the magnetic field, because $\beta = 8\pi nkT/B^2 \ll 1$ in the whole numerical region. The levels of

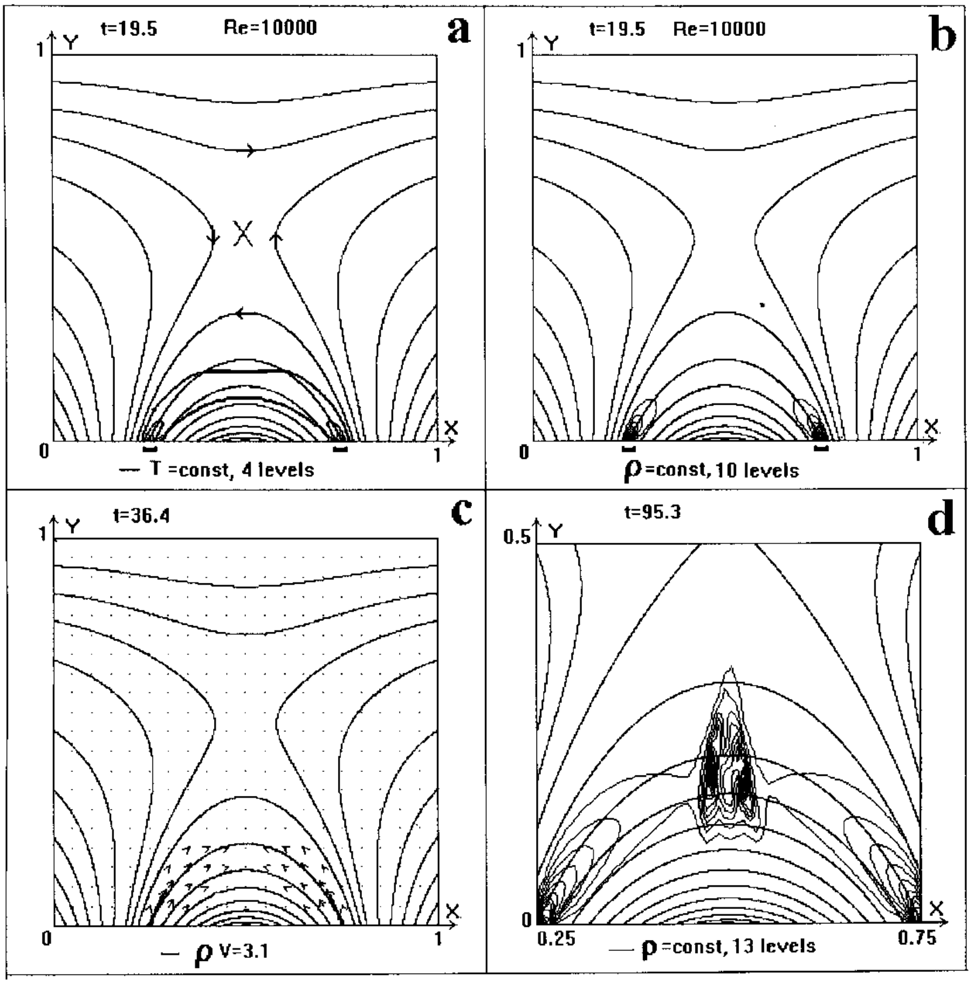

FIGURE 2 Loops filling by plasma from chromospheric evaporation. (a) The postflare magnetic configuration, levels of T = constant and the positions of sources are shown. (b) Magnetic lines and density levels. (c) Plasma flux vectors. (d) Density levels for a later time.

$T = \text{constant}$ (thick lines) are also presented in this picture for the time $t = 19.5$. Between the levels, $\Delta T = 2.5$. The heat propagates along the field lines because of the high ratio of thermal conductivity anisotropy in the magnetic field. Figure 2(b) shows the plasma density levels for the same time $t = 19.5$. Plasma also moves along the field lines, filling the loop. It is seen that plasma heating propagates ahead of the motion of matter because of the high plasma thermal conductivity along the field lines. Later, the plasma streams meet at the loop top (Figs. 2(c) and (d)).

4 LOOP TOP HEATING

During a solar flare the plasma temperature increases owing to reconnection. Simultaneously, plasma is accelerated along the sheet by the force of magnetic stretching (Podgorny and Podgorny, 2001a). The plasma accelerated upwards produces coronal mass ejection. The downward acceleration of plasma is not so effective, because the downward flux meets a strong arc field. The flux of hot plasma from the CS results in reconnected field lines. These lines are piled up on the top of the loop. As a result, the outer part of the loop becomes hotter than its inner part. This temperature distribution is typical for postflare loops (Schmieder et al., 1996). The concentration of reconnected magnetic lines and hot plasma on the loop top can produce the effect of increasing loop luminosity. However, this effect is not associated with the matter rising upwards but is determined by the downward flow of the hot plasma. The plasma flow to the Sun from the region of reconnection has been observed by McKenzie and Hudson (2001). They have called this phenomenon ‘supra-arcade downflow’.

5 LOOP STABILITY AND FIELD-ALIGNED CURRENT GENERATION

Many observation data show that a loop has a stable existence for several hours. It seems that these data contradict numerous results of laboratory experiments with thermonuclear adiabatic magnetic traps. In a laboratory trap with axial symmetry the magnetic field decreases along the radius. The strongest instability in such a magnetic field is the flute instability.

In the case of total symmetry the particles drift in the magnetic field gradient along a circular trajectory. The electrons and ions drift in opposite directions. They produce a closed current, but no charge accumulation occurs (Fig. 3(a)). The directions of the drift velocities V_{de} and V_{di} are shown in the figure. However, if a prominence accidentally appears, the drift trajectory inside is no longer closed, and electrical charges are accumulated on the prominence borders. The electric field E appears. Now the drift velocity $V = cE \times B/B^2$ in the electric and magnetic fields is directed upwards for all particles, and plasma escapes from the trap. This instability does not permit plasma confinement for a long time.

Inside a loop the magnetic field gradient is directed upwards (Fig. 3(b)). Here drift currents are not closed. They produce charge separation, and an electric field appears that should initiate all loops to move upwards with acceleration $dV/dt = k(T_i + T_e)/m_iR$ (Rosenbluth and Longmire, 1957). Here R is the magnetic line radius and m_i is the mass of ion.

At a plasma density $n \approx 10^8\,\text{cm}^{-3}$, a temperature $T \approx 1000\,\text{eV}$ and a loop curvature radius $R \approx 10^{10}\,\text{cm}$, the time of the loop escape from an active region should be of the order of 100 s. However, this mechanism does not work in the corona, because both legs of a loop are located in the dense chromospheric plasma. In this case, electrons can move along the magnetic lines, producing a FAC. This FAC compensates induced electric charges. So, the FACs suppress the instability.

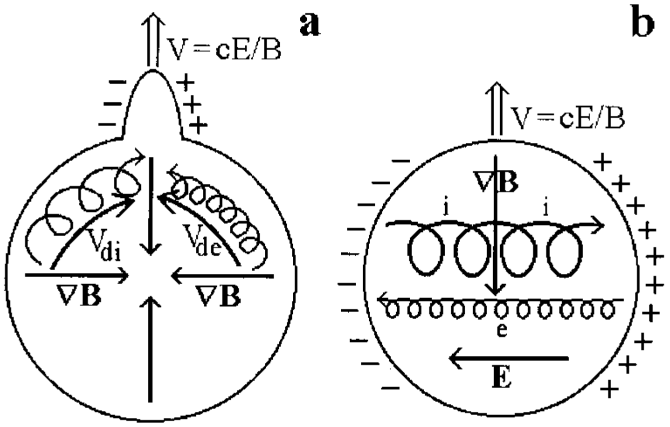

FIGURE 3 Electron and ion drifts in the magnetic field gradient in a symmetrical adiabatic trap and in the magnetic arch.

The FAC density can be estimated. The velocity of particle drift in a loop in the direction perpendicular to the magnetic field and its gradient is $V_d \approx ckT/eBR \approx 10^8 T$ (eV)/BR. At $T = 1$ keV, $B = 100$ G and $R = 10^{10}$ cm the drift velocity is 10^{-1} cm s^{-1}. The ions and electrons drift in opposite direction perpendicular to the loop plane. They produce a current $j_\perp = 2neV_d$. At $n = 10^9$ cm^{-3}, $j_\perp \approx 3 \times 10^{-11}$ A cm^{-2}. Using div $j = 0$, one can obtain the linear density of the FAC that flows in the chromosphere. Near the chromosphere it is of the order of 0.5 A cm^{-1}.

6 LONG-DURATION EVENTS

After a short pulse of hard X-rays, the long duration of soft X-rays, visible and ultraviolet emission are usually observed. The IV type of radio emissions that occur at cyclotron frequencies reveals similar behaviour. Electrons with an energy of about 10 keV produce these effects. These electrons gain their energy in the reconnection site. They arrive at the loop top during reconnected the contraction of magnetic field lines. The electrons are confined in the arch magnetic field as in an adiabatic trap. All electrons with the angle between the velocity vector and the magnetic line given by $\alpha >$ arcsin $[(B_0/B_{max})^{1/2}]$ cannot escape from the loop. Here B_0 and B_{max} are the magnetic fields in the loop centre and in the loop legs near the chromosphere respectively. Electrons slowly precipitate in the chromosphere owing to adiabatic invariant violation. The confinement time $\tau \approx 5 \times 10^4 (T\ \mathrm{eV})^{3/2}/n$ of hot electrons in a loop is determined by electron Coulomb scattering, which transfers the velocity vector into a cone of losses. As a result the electrons escape the loop and hence hit the chromosphere. The confinement time for an electron energy of 10 keV and a density of 2×10^7 cm^{-3} is about 1 h.

7 CONCLUSION

Loop filling by a plasma due to chromospheric evaporation is demonstrated in the numerical MHD experiments. Anisotropy of the thermal conductivity of the plasma in the magnetic field is taken into account. The heating of the loop top can be explained by magnetic reconnection in a vertical CS above a postflare loop. The long stable plasma confinement in the arch magnetic field is supplied by induced electric charge leakage into the chromosphere. As a result, FACs appear. The stable confinement of electrons in a loop is responsible for long-duration events.

Acknowledgements

The new version of PERESVET code was developed with the support of the Russian Basic Research Foundation (Grants 01-02-16186 and 00-01-00091) and the Russian State Program Astronomoya.

References

Culhane, J. L., Phillips, A. T., Inda-Koide, M., Kosugi, T., Fludra, A., Kurokawa, H., Makishima, K., Pike, C. D., Sakao, T., Sakurai, T. (1994). Solar Phys., 153, 307.
Fisher, G. H., Canfield, R. C. and McClimon, A. N. (1985). Astrophys. J., 289, 414.
McKenzie, D. E. and Hudson, H. S. (2001). Earth Planet. Space, 53, 577.
Podgorny, A. I. and Podgorny, I. M. (2001a). Astron. Rep., 45, 60.
Podgorny, A. I. and Podgorny, I. M. (2001b). Astron. Astrophys. Trans., 20, 559.
Podgorny, A. I. and Podgorny, I. M. (2001c). Solar Phys., 182, 159.
Podgorny, A. I. and Podgorny, I. M. (2002). Astron. Rep., 46, 65.
Rosenbluth, M. and Longmire, C. (1957). Ann. Phys. NY, 1, 120.
Schmieder, B., Heinzel, P., van Dril-Gesztelyi, L. and Lemon, J. R. (1996). Solar Phys., 165, 303.